DIRECTIONAL DECOMPOSITION BASED TOTAL VARIATION IMAGE RESTORATION

Daniel R. Pipa[1], *Stanley H. Chan*[2] *and Truong Q. Nguyen*[3]

[1]Universidade Federal do Rio de Janeiro (COPPE/UFRJ) - Contacting author: danielpipa@gmail.com
[2]Harvard University - School of Engineering and Applied Science
[3]University of California, San Diego - Department of Electrical and Computer Engineering

ABSTRACT

This paper proposes an extension of total variation (TV) image deconvolution technique that enhances image quality over classical TV while preserving algorithm speed. Enhancement is achieved by altering the regularization term to include *directional decompositions* before the gradient operator. Such decompositions select areas of the image with characteristics that are more suitable for a certain type of gradient than another. Speed is guaranteed by the use of the augmented Lagrangian approach as basis for the algorithm. Experimental evidence that the proposed approach improves TV deconvolution is provided, as well as an outline for a future work aiming to support and substantiate the proposed method.

Index Terms— Total variation, augmented Lagrangian, image deconvolution, image restoration, directional decompositions.

1. INTRODUCTION

Image deconvolution/restoration is a classic inverse problem that has been extensively studied in the literature. In such problems, one aims to recover a clean, sharp image from a noisy, blurred and/or degraded observation. The challenge of most inverse problems is that they are ill-posed, i.e., either the direct operator does not have an inverse, or it is nearly singular. Thus, regularization is required to deal with noise and ensure a unique solution [1].

Since its introduction in 1992 by Rudin, Osher and Fatemi [2], Total Variation (TV) regularization has been successfully applied to a variety of deconvolution-related image problems [1]. The success of TV regularization relies on a good balance between the ability to describe piecewise smooth images (without penalizing possible discontinuities) and the complexity of the resulting algorithms [3].

To go on with the idea, let $\mathbf{f}$ be a vector representing an unknown image (to be predicted) lexicographically ordered, which is observed through the model

$$\mathbf{g} = \mathbf{H}\mathbf{f} + \boldsymbol{\eta} \tag{1}$$

giving rise to a blurred and noisy image $\mathbf{g}$. The blur operator is represented by $\mathbf{H}$ and $\boldsymbol{\eta}$ is the noise term such that $\boldsymbol{\eta} \sim \mathcal{N}(\mathbf{0}, \sigma^2\mathbf{I})$. We are interested in estimating $\mathbf{f}$ given $\mathbf{g}$ and $\mathbf{H}$.

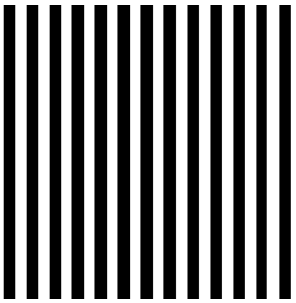

Fig. 1. A toy example showing that classical TV can be improved by choosing appropriate β_x and β_y.

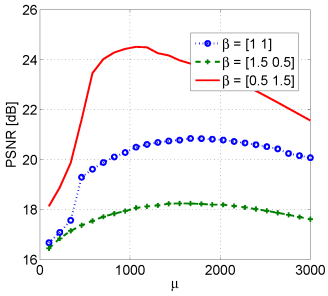

Fig. 2. PSNR is maximized when $\boldsymbol{\beta}$ is biased towards the vertical direction.

To solve (1) we apply the total variation (TV) approach

$$\hat{\mathbf{f}} = \underset{\mathbf{f}}{\operatorname{argmin}} \frac{\mu}{2}\|\mathbf{H}\mathbf{f} - \mathbf{g}\|^2 + TV(\mathbf{f}), \tag{2}$$

where μ is the regularization parameter, $TV(\mathbf{f}) = \|\mathbf{D}\mathbf{f}\|_1$ is the anisotropic total variation norm on $\mathbf{f}$ and $\mathbf{D}$ is the classical gradient operator such that

$$\mathbf{D}\mathbf{f} = \begin{bmatrix}\beta_x\mathbf{D}_x \\ \beta_y\mathbf{D}_y\end{bmatrix}\mathbf{f}, \tag{3}$$

with $\mathbf{D}_x = [-1,\ 1]$ and $\mathbf{D}_y = [-1,\ 1]^{\mathrm{T}}$. Here, β_x and β_y, sometimes grouped as $\boldsymbol{\beta} = [\beta_x,\ \beta_y]^{\mathrm{T}}$, are constants that control the amount of horizontal and vertical regularization, respectively. For instance, if the real image $\mathbf{f}$ is expected to have some "vertical" pattern, i.e. Figure 1, the reconstruction process should penalize preferably vertical frequencies by choosing $\beta_y > \beta_x$.

As an example, we simulated an observation of Figure 1 by blurring it with a 9×9 Gaussian kernel with $\sigma = 3$ and adding noise up to BSNR[1] = 25dB. Then, we deblurred it using the approach on (2) for different choices of the regularization parameter μ. Figure 2 shows the evolution of the PSNR

[1]Blurred Signal to Noise Ratio = 10 log (Blurred signal variance / Noise variance) [dB].

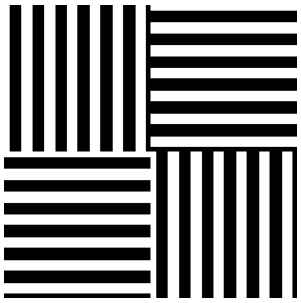

Fig. 3. A less simple toy example. Altering β_y and/or β_x does not yield better PSNR.

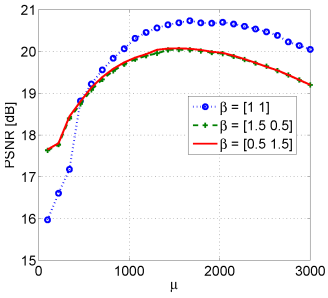

Fig. 4. Since the figure has a mixed pattern, the best result is achieve using a balanced $\boldsymbol{\beta}$.

for some choices of $\boldsymbol{\beta}$. The choice $\boldsymbol{\beta} = [0.5,\ 1.5]$, based on previous knowledge about the real image, forces the solution to have more horizontal than vertical frequency content, resulting in better image quality and higher PSNR.

However, when the real image does not have a preferable frequency pattern, i.e. Figure 3, no PSNR increment is achieve by altering $\boldsymbol{\beta}$, as shown on Figure 4. In this paper, we address this issue.

This paper is organized as follows: Section 2 reviews previous work on extending TV deconvolution for images. In Section 3 we briefly describe the augmented Lagrangian approach and highlight the characteristics that yields efficient implementation. Finally, the proposed method is explained in details in Section 4.

2. RELATED WORK

Many extensions of TV have been reported in the literature [4]. Most of them [5–7] deals with the *staircase effect*, namely the transformation of smooth regions (ramps) into piecewise constant regions (stairs). Such a phenomenon tends to appear when trying to reconstruct, say, a piecewise smooth image (rather than a piecewise constant image) using classical TV.

For this purpose, Chambolle and Lions proposed the use of a second order variation along with the traditional TV in [5]. In [6] Chan et al. improved the approach of [5] by considering texture and structure as separate components of an image. Stefan et al. used a variable order total variation approach in [7]. The order is chosen after an edge detection procedure.

In [8] Farsiu et al. introduced a technique called Bilateral TV, which they apply to solve a super-resolution problem [9]. Basically, rather than calculating only first-order finite differences, which is often used to approximate the gradient operator [2], they use a weighted mean of combinations of horizontal and vertical differences. As a result, not only horizontal and vertical differences are computed, but also diagonal differences.

Kiriyama et al., in [10], proposed to speed up the Chambolle's projected method [11] by adding diagonal differences to the TV regularization term. They reported a reduction in computational time around 56% (as a result of fewer iterations).

In [12] Karahanoğlu et al. proposed the use of a general differential operator $\mathbf{L}$ instead of the derivative $\mathbf{D}$ for 1-D signal processing. Specifically, $\mathbf{L}$ can be tuned according to the expected signal and the presence of a linear system.

Differently from the previously proposed techniques, our approach uses directional filters to decompose the image into directional components. Then, we apply the appropriate gradient operator on each component, thus penalizing only the undesired directional patterns.

3. AUGMENTED LAGRANGIAN METHOD

The problem in (2) can be solved efficiently using the augmented Lagrangian approach [13, 14]. The idea consists of introducing intermediate variables $\mathbf{u}$ and transforming the unconstrained optimization problem in (2) into the equivalent constrained problem

$$\begin{aligned} &\underset{\mathbf{f},\mathbf{u}}{\text{minimize}}\ \frac{\mu}{2}\|\mathbf{Hf}-\mathbf{g}\|^2+\|\mathbf{u}\|_1 \\ &\text{subject to}\ \ \mathbf{u}=\mathbf{Df}. \end{aligned} \tag{4}$$

The resulting problem is then solved using an augmented Lagrangian (AL) scheme [13–15]

$$\begin{aligned} L(\mathbf{f},\mathbf{u},\mathbf{y}) = \frac{\mu}{2}\|\mathbf{Hf}-\mathbf{g}\|^2+\|\mathbf{u}\|_1 - \\ -\mathbf{y}^{\mathrm{T}}(\mathbf{u}-\mathbf{Df})+\frac{\rho_r}{2}\|\mathbf{u}-\mathbf{Df}\|^2, \end{aligned} \tag{5}$$

where ρ_r is a regularization parameter associated with the quadratic penalty term $\|\mathbf{u}-\mathbf{Df}\|^2$, and $\mathbf{y}$ is the Lagrange multiplier associated with the constraint $\mathbf{u}=\mathbf{Df}$.

The idea of the augmented Lagrangian method is to find a saddle point of $L(\mathbf{f},\mathbf{u},\mathbf{y})$ that is also the solution of the original problem (2). To this end, the alternating direction method of multipliers (ADMM) can be used to solve the following sub-problems iteratively [14]:

$$\begin{aligned} \hat{\mathbf{f}}_{k+1} = \underset{\mathbf{f}}{\operatorname{argmin}}\ \frac{\mu}{2}\|\mathbf{Hf}-\mathbf{g}\|^2 \\ -\hat{\mathbf{y}}_k^{\mathrm{T}}(\hat{\mathbf{u}}_k-\mathbf{Df})+\frac{\rho_r}{2}\|\hat{\mathbf{u}}_k-\mathbf{Df}\|^2 \end{aligned} \tag{6}$$

$$\begin{aligned} \hat{\mathbf{u}}_{k+1} = \underset{\mathbf{u}}{\operatorname{argmin}}\|\mathbf{u}\|_1-\hat{\mathbf{y}}_k^{\mathrm{T}}(\mathbf{u}-\mathbf{D}\hat{\mathbf{f}}_{k+1}) \\ +\frac{\rho_r}{2}\|\mathbf{u}-\mathbf{D}\hat{\mathbf{f}}_{k+1}\|^2 \end{aligned} \tag{7}$$

$$\hat{\mathbf{y}}_{k+1} = \hat{\mathbf{y}}_k-\rho_r(\hat{\mathbf{u}}_{k+1}-\mathbf{D}\hat{\mathbf{f}}_{k+1}). \tag{8}$$

Now, the $\mathbf{f}$-subproblem in (6) has a closed-form solution and can be efficiently calculated through FFT [14]. The $\mathbf{u}$-subproblem in (7) can be solved using the shrinkage formula

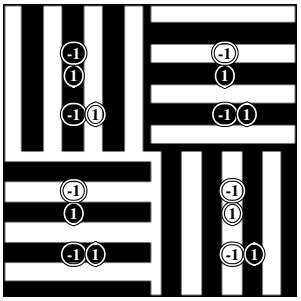

Classical TV penalizes variations over the whole image in vertical (top) and horizontal (bottom circles) directions. For numbers with same colour, gradient is zero (null penalization), whereas different colours cause penalization. Thus, image patterns such as stripes are penalized.

Fig. 5. An illustration of gradient calculation in classical TV

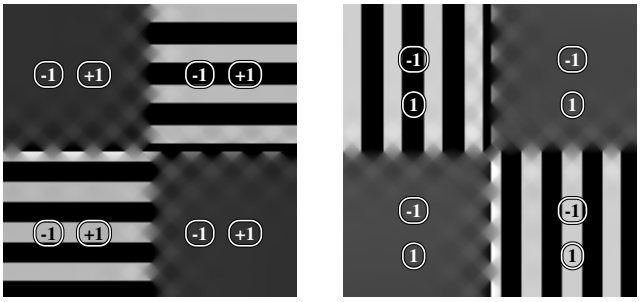

Fig. 6. Gradients applied to image *components* in the proposed method. Penalization of image features is minimum since gradient is close to zero.

[16] at very low cost, as well as the $\mathbf{y}$-subproblem in (8), which consists of a mere update.

4. PRE-FILTERING/DECOMPOSING APPROACH

The algorithm we have just described uses classical TV approach, where the gradient operator $\mathbf{D}$ is applied to all regions of the image (Figure 5). As a consequence, variations are penalized in all directions.

As observed in Section 1, however, we can improve TV deconvolution by using a tuned gradient operator. Rather than using masks to select regions of the image that are better suited for a certain gradient operator, we will use pre-filters to perform such a task. The advantage of the proposed approach is that it maintains the block-circulant structure of the matrices involved allowing the use of fast algorithms.

Any image $\mathbf{f}$ can be decomposed as

$$\mathbf{f} = \mathbf{f}_x + \mathbf{f}_y, \tag{9}$$

where $\mathbf{f}_x$ represent the "horizontal" content or component of $\mathbf{f}$ and $\mathbf{f}_y$ "vertical" component. The components $\mathbf{f}_x$ and $\mathbf{f}_y$ are computed as

$$\mathbf{f}_x = \mathbf{B}_x\mathbf{f} \quad \text{and} \quad \mathbf{f}_y = \mathbf{B}_y\mathbf{f}, \tag{10}$$

where $\mathbf{B}_x$ and $\mathbf{B}_y$ are block-circulant matrices with the property that $\mathbf{I} = \mathbf{B}_x + \mathbf{B}_y$. Therefore,

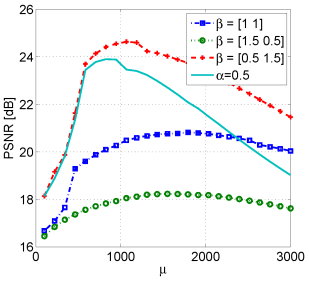

Fig. 7. Proposed method ($\alpha = 0.5$) provides results comparable to tuned classical TV restoration for the toy example of Figure 1.

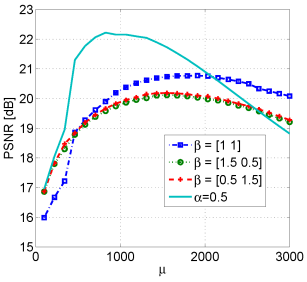

Fig. 8. For the mixed pattern of Figure 3, the proposed method outperforms any combination of $\boldsymbol{\beta}$ in the classical TV.

$$\mathbf{D}\mathbf{f} = \mathbf{D}(\mathbf{B}_x + \mathbf{B}_y)\mathbf{f} \tag{11}$$

$$= \left(\begin{bmatrix} \beta_x \mathbf{D}_x \mathbf{B}_x \\ \beta_y \mathbf{D}_y \mathbf{B}_x \end{bmatrix} + \begin{bmatrix} \beta_x \mathbf{D}_x \mathbf{B}_y \\ \beta_y \mathbf{D}_y \mathbf{B}_y \end{bmatrix} \right) \mathbf{f}. \tag{12}$$

We observe in (12) that the gradient operators are now applied to filtered versions of $\mathbf{f}$, though the effect has not changed due to identity $\mathbf{I} = \mathbf{B}_x + \mathbf{B}_y$. Since we want $\mathbf{D}_x$ to operate on the "horizontal" portion of $\mathbf{f}$ and $\mathbf{D}_y$ on its "vertical" counterpart, we replace β_x and β_y which yields

$$\mathbf{D}_{2D}\mathbf{f} = \left(\begin{bmatrix} \frac{(1+\alpha)}{2} \mathbf{D}_x \mathbf{B}_x \\ \frac{(1-\alpha)}{2} \mathbf{D}_y \mathbf{B}_x \end{bmatrix} + \begin{bmatrix} \frac{(1-\alpha)}{2} \mathbf{D}_x \mathbf{B}_y \\ \frac{(1+\alpha)}{2} \mathbf{D}_y \mathbf{B}_y \end{bmatrix} \right) \mathbf{f} \tag{13}$$

with

$$0 \leq \alpha \leq 1 \tag{14}$$

α controls the "adaptiveness". Now, when $\alpha = 0$ we have the traditional TV regularization equivalent to $\beta_x = \beta_y = 1$, whereas when $\alpha = 1$, $\mathbf{D}_x$ is applied only to $\mathbf{B}_x\mathbf{f}$ and $\mathbf{D}_y$ only to $\mathbf{B}_y\mathbf{f}$.

Simulations have shown that the choice of α should take into account the noise level. When noise is high, for instance, regularization should be less "adaptive" and setting α close to 1 will produce poor results. The intuition is that noise corrupts direction patterns, making it hard to select/filter for the use of a specific gradient in restoration.

Finally, the proposed algorithm is obtained by replacing $\mathbf{D}\mathbf{f}$ in equations (4) through (8) by $\mathbf{D}_{2D}\mathbf{f}$ in (13). Refer to [17] for algorithmic details.

4.1. Choice of filters

Since we want horizontal and vertical image components, a straightforward solution is to split the 2-D spectrum in horizontal ($|\omega_x| > |\omega_y|$) and vertical ($|\omega_x| < |\omega_y|$) frequencies

and define the Fourier transforms of the filters from this partition as

$$|B_x(e^{j\omega_x}, e^{j\omega_y})| = \begin{cases} 0 & \text{if } |\omega_x| > |\omega_y| \\ \frac{1}{2} & \text{if } |\omega_x| = |\omega_y| \\ 1 & \text{if } |\omega_x| < |\omega_y| \end{cases} \quad (15)$$

and $|B_y(e^{j\omega_x}, e^{j\omega_y})| = 1 - |B_x(e^{j\omega_x}, e^{j\omega_y})|$. Then, the filters were designed through Matlab function `fwind1`, which uses the window method [18].

Figure 6 illustrates the idea of the proposed method. After selecting regions of the image with filters, only the appropriate gradient is applied. Thus, image features are minimally penalized.

Figures 7 and 8 show the PSNR evolution of the proposed algorithm versus the classical approach for the images on Figures 1 and 3 respectively.

4.2. 4-direction TV deconvolution

Simulations have shown that the approach we have just described is insufficient to enhance TV deconvolution for real images. We now extend the idea to incorporate diagonal gradients in addition to horizontal and vertical gradients by defining the following.

The $\mathbf{D}_{4D}$ operator in the regularization term becomes

$$\left(\begin{bmatrix} \gamma\mathbf{D}_x\mathbf{B}_x \\ \delta\mathbf{D}_y\mathbf{B}_x \\ \delta\mathbf{D}_w\mathbf{B}_x \\ \delta\mathbf{D}_z\mathbf{B}_x \end{bmatrix} + \begin{bmatrix} \delta\mathbf{D}_x\mathbf{B}_y \\ \gamma\mathbf{D}_y\mathbf{B}_y \\ \delta\mathbf{D}_w\mathbf{B}_y \\ \delta\mathbf{D}_z\mathbf{B}_y \end{bmatrix} + \begin{bmatrix} \delta\mathbf{D}_x\mathbf{B}_w \\ \delta\mathbf{D}_y\mathbf{B}_w \\ \gamma\mathbf{D}_w\mathbf{B}_w \\ \delta\mathbf{D}_z\mathbf{B}_w \end{bmatrix} + \begin{bmatrix} \delta\mathbf{D}_x\mathbf{B}_z \\ \delta\mathbf{D}_y\mathbf{B}_z \\ \delta\mathbf{D}_w\mathbf{B}_z \\ \gamma\mathbf{D}_z\mathbf{B}_z \end{bmatrix} \right) \quad (16)$$

with

$$\gamma = 1 + \alpha, \quad \delta = 1 - \alpha \quad \text{and} \quad 0 \leq \alpha \leq 1. \quad (17)$$

The gradient matrices $\mathbf{D}_x$ through $\mathbf{D}_z$ perform the differences defined respectively by the kernels (filter coefficients)

$$d_x = \begin{bmatrix} -1 & 1 \end{bmatrix} \qquad d_y = \begin{bmatrix} -1 \\ 1 \end{bmatrix} \quad (18)$$

$$d_w = \begin{bmatrix} 0 & 1 \\ -1 & 0 \end{bmatrix} \qquad d_z = \begin{bmatrix} -1 & 0 \\ 0 & 1 \end{bmatrix}. \quad (19)$$

The filters can be easily defined by partitioning the spectrum similarly to (15) and are summarized in Table 1. As observed, the filters are more selective than those defined in Section 4.1.

Figures 9 through 14 (zoomed-in versions of Cameraman, Mandrill and Lena, respectively) show real image results of the proposed 4-direction TV deconvolution algorithm compared to traditional TV deconvolution. Prior to restoration, the images were blurred with a 9×9 Gaussian kernel with $\sigma = 1.8$ and corrupted with noise $\mathcal{N}(0; 3 \times 10^{-5})$ (image dynamic range is $0 \sim 1$). The parameter α was empirically set to 0.5.

$\lvert B_x\rvert = 0$ if $\lvert 2\omega_x\rvert > \lvert\omega_y\rvert$, $\lvert B_x\rvert = 1$ otherwise
$\lvert B_y\rvert = 0$ if $\lvert\omega_x\rvert < \lvert 2\omega_y\rvert$, $\lvert B_y\rvert = 1$ otherwise
$\lvert B_w\rvert = 1$ if $\omega_x < 2\omega_y < 4\omega_x$ or $\omega_x > 2\omega_y > 4\omega_x$ $\lvert B_w\rvert = 0$ otherwise
$\lvert B_z\rvert = 1$ if $\omega_y < 2\omega_x < 4\omega_y$ or $\omega_y > 2\omega_x > 4\omega_y$ $\lvert B_z\rvert = 0$ otherwise

Table 1. Filters for the 4-direction TV deconvolution. Additionally, $|B| = 1/2$ on the boundaries for all filters.

Fig. 9. Classical: 83.15 dB

Fig. 10. Proposed: 84.23 dB

5. CONCLUSION

In this paper, we proposed and showed results of an extension of the augmented Lagrangian approach [13, 14] for the problem of image deconvolution.

We started our development by noting that unbalancing the amount of horizontal and vertical regularization enhances classical TV deconvolution if the original image has a preferred frequency content, although the same is not true for more complex images.

In order to deal with a wider range of images, we recognized that different regions of the image require different regularizations. Rather than using masks to achieve this selection, we introduced directional decompositions/filters to perform this task. The advantage of the latter is that it permits the use of fast FFT-based algorithms due to block-circulant nature of matrices involved.

Fig. 11. Classical: 76.92 dB

Fig. 12. Proposed: 77.35 dB

Fig. 13. Classical: 77.74 dB

Fig. 14. Proposed: 78.31 dB

Even for high vertical or horizontal images, our method has advantages because it does not require any previous knowledge about the image. For classical TV, on the other hand, one has to set the amount of horizontal and vertical regularization accordingly to the image.

We presented experiments showing better PSNR and visual quality of the proposed method over the classical TV deconvolution, while increasing only slightly computational complexity.

Future work includes:

- Deduce the decomposition filters from a certain criterion, rather than defining them arbitrarily;
- Provide analytical analyses of our method;
- Study computational complexity increment caused by increasing number of filters (e.g. more than 4 filters);
- Include a procedure for automatic parameter selection (parameters μ and α);
- Take advantage of the directional nature of our method and add an interpolation step/operation for extension to the problem of super-resolution/interpolation.

6. REFERENCES

[1] M. Bertero and P. Boccacci, *Introduction to Inverse Problems in Imaging*, IOP Pub., Bristol, UK, 1998.

[2] L. I. Rudin, S. Osher, and E. Fatemi, "Nonlinear total variation based noise removal algorithms," *Physica D.*, vol. 60, pp. 259–268, 1992.

[3] J. M. Bioucas-Dias, M. A. T. Figueiredo, and J. P. Oliveira, "Adaptive total variation image deconvolution: A majorization-minimization approach," in *Proc. EUSIPCO*, 2006.

[4] T. Chan, S. Esedoglu, F. Park, and A. Yip, *Handbook of Mathematical Models in Computer Vision*, chapter 2 - Total Variation Image Restoration: Overview and Recent Developments, Springer, New York, 2005.

[5] A. Chambolle and P. L. Lions, "Image recovery via total variation minimization and related problems," *Numer. Math.*, vol. 76, pp. 167–188, 1997.

[6] T. F. Chan, S. Esedoglu, and F. E. Park, "Image decomposition combining staircase reduction and texture extraction," *J. Vis. Comun. Image Represent.*, vol. 18, pp. 464–486, Dec. 2007.

[7] W. Stefan, R. Renaut, and A. Gelb, "Improved total variation-type regularization using higher order edge detectors," *SIAM J. Imag. Sci.*, pp. 232–251, Jan. 2010.

[8] S. Farsiu, M. D. Robinson, M. Elad, and P. Milanfar, "Fast and robust multiframe super resolution," *IEEE Trans. on Image Processing*, vol. 13, no. 10, pp. 1327–1344, Oct. 2004.

[9] S. Park, M. K. Park, and M. G. Kang, "Super-resolution image reconstruction: a technical overview," *IEEE Signal Proc. Magazine*, vol. 20, no. 3, pp. 21–36, 2003.

[10] S. Kiriyama, T. Usui, T. Goto, S. Hirano, M. Sakurai, and T. Saito, "Diagonal total variation regularization criterion for fast convergence," in *Proc. ICALIP*, Nov. 2010, pp. 1494–1498.

[11] A. Chambolle, "An algorithm for total variation minimization and applications," *J. of Math. Imaging and Vision*, vol. 20, no. 1–2, pp. 89–97, 2004.

[12] F. I. Karahanoğlu, İlker Bayram, and D. V. D. Ville, "A signal processing approach to generalized 1-d total variation," *IEEE Trans. on Signal Processing*, vol. 59, pp. 5265–5274, Nov. 2011.

[13] M. Afonso, J. Bioucas-Dias, and M. Figueiredo, "Fast image recovery using variable splitting and constrained optimization," *IEEE Trans. on Image Processing*, vol. 19, pp. 2345–2356, Sep. 2010.

[14] S. H. Chan, R. Khoshabeh, K. B. Gibson, P. E. Gill, and T. Q. Nguyen, "An augmented Lagrangian method for total variation video restoration," *IEEE Trans. on Image Processing*, vol. 20, no. 11, pp. 3097–3111, Nov. 2011.

[15] J. Nocedal and S. J. Wright, *Numerical Optimization*, Springer-Verlag, New York, 2nd edition, 2006.

[16] C. Li, "An efficient algorithm for total variation regularization with applications to the single pixel camera and compressive sensing," M.S. thesis, Rice University, Sep. 2009.

[17] `http://sites.google.com/site/danielpipa/ /papers/conference/eusipco2012`.

[18] P. S. R. Diniz, E. A. B. da Silva, and S. L. Netto, *Digital Signal Processing: System Analysis and Design*, Cambridge University Press, Cambridge, 2nd edition, 2010.